

On irregularities in the cosmic ray spectrum of $10^{16} - 10^{18}$ eV range.

S. P. Knurenko and I. S. Petrov^{*}

Yu. G. Shafer Institute of Cosmophysical Research and Aeronomy, Yakutsk, Russia

^{*} igor.petrov@mail.ysn.ru

August 12, 2022



21st International Symposium on Very High Energy Cosmic Ray Interactions
(ISVHE- CRI 2022)

Online, 23-28 May 2022

doi:[10.21468/SciPostPhysProc.7](https://doi.org/10.21468/SciPostPhysProc.7)

Abstract

Small, medium and large arrays for the study of cosmic rays of ultra-high energies existing are aimed at obtaining information about our Galaxy and metagalactic space. Concretely search and study of astronomical objects, that forms flux of relativistic particles that fill outer space. The drift and interaction of such particles with magnetic field and shock waves taking place in interstellar space causes the same interest. The shape of the energy spectrum of cosmic rays in the energy range $10^{15} - 10^{18}$ eV, where "knee" and "second knee" is observed, can be formed as a superposition of the partial spectra of various chemical elements. Verification of galactic models, using recent experimental spectral data, makes it possible to study the nature of the galactic and metagalactic components of cosmic rays. The paper presents the result of the energy spectrum of cosmic rays in the range $10^{16} - 10^{18}$ eV measurements obtained at the Small Cherenkov array — a part of the Yakutsk array.

1 Introduction

The main objectives of ultra-high energy cosmic ray (CR) studies are to determine the anisotropy, energy spectrum, and chemical composition of primary CR particles. These characteristics of cosmic rays play an important role in understanding the origin, acceleration, and propagation of primary particles of different energies. In the energy range of $10^{12} - 10^{14}$ eV, such measurements are performed on satellites [1–3] and by launching balloons to altitudes of 35 km [4, 5]. In these experiments, it is possible to directly measure both the chemical composition of the particles and their partial spectra. The only drawback of such experiments is the small luminosity of the lifted detectors and the limited observation time. At energies greater than 10^{14} eV due to low intensity cosmic rays can be studied only by extensive air showers (EAS), i.e. indirectly, by tracking the cascade processes in the atmosphere and detecting the charged particles fluxes, muons, ionization luminescence and Cherenkov light of air showers at sea level. Due to the very wide spectrum of cosmic rays, arrays with variety of sizes are employed: compact ones with an area of $s < 1 \text{ km}^2$ that registers air showers up to energies of 10^{18} eV, average sized arrays with $s < 20 \text{ km}^2$ — up to energies of 10^{19} eV and huge arrays such as Auger [6], Telescope Array [7] for higher energies.

2 Small Cherenkov Array

In 1994, a Small Cherenkov array was created on the basis of the central part of the Yakutsk array to register EAS of moderate energies (Fig. 1). Distinctive feature of the Small Cherenkov is that it measures several components of EAS like muons, electrons and Cherenkov radiation unlike other compact arrays like KASCADE [8] or TUNKA [9]. This allows a broader look at the development of the shower, including longitudinal development, registering the spatial distribution of electrons, muons and EAS Cherenkov light at sea level [10, 11] and its longitudinal profile using the measurement of the flux of Cherenkov photons (which are generated throughout development of the shower in the atmosphere) by integral and differential Cherenkov detectors [11, 12].

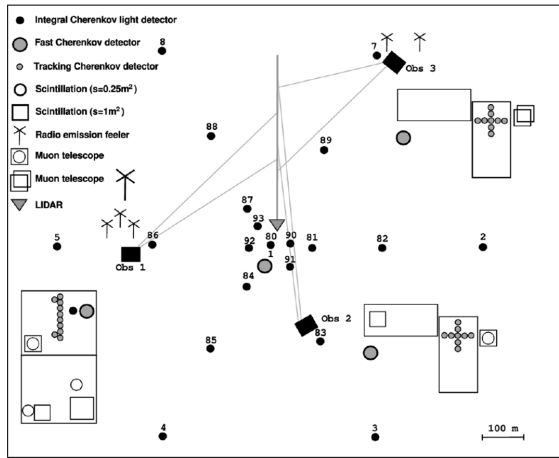


Figure 1: The layout of the detectors of charged particles, muons, and Cherenkov light on the Small Cherenkov array located in the center of the Yakutsk array

3 Air Shower Measurement Simulation at the Small Cherenkov Array

To estimate the precision of determining air shower characteristics at the Yakutsk array, full Monte Carlo simulation was carried out. The simulation results are shown in Table 1.

Table 1: E_0 — air shower energy [PeV]; $\sigma(R)$ — axis reconstruction error [m]; δN_s — total number of charged particles determination error, $\sigma(Q(100))$, $\sigma(Q(200))$ and $\sigma(Q(400))$ — errors of determining the classification parameters of the Cherenkov radiation flux at a distance 100, 200 and 400 m respectively [phot./m^2]; $\sigma(\rho_s(300))$ and $\sigma(\rho_s(600))$ — errors of determining of total charged particles flux density at 300 and 600 m respectively [$1/\text{m}^2$]; θ — zenith angle determination uncertainty [°]

E_0	$\sigma(R)$	δN_s	$\sigma(Q(100))$	$\sigma(Q(200))$	$\sigma(Q(400))$	$\sigma(\rho_s(300))$	$\sigma(\rho_s(600))$	θ
2	9.7	0.15	0.17	-	-	-	-	1.3
10	7.2	0.11	0.15	-	-	-	-	1.0
100	15.5	0.27	0.15	0.25	-	-	-	1.7
200	14.6	0.32	0.20	0.20	0.22	0.25	-	1.4
1000	16.7	0.35	-	-	0.20	0.17	0.19	1.3

In a real atmosphere, there is always a noticeable contribution of light loss on aerosol particles of different sizes. In addition, the uncertainty is also caused by the extreme continental climate in the array region, i.e. in winter a non-standard atmosphere is formed above the array, the parameters that differ significantly from the atmosphere during summer period. As it was shown in the papers [12, 14] in winter, with near-ground mists and haze, the maximum flux attenuation of Cherenkov light at distances of 100–400 m from the shower axis reaches $\sim (30\text{--}40)\%$, while under excellent weather conditions the losses do not exceed 10%, which occurs due to Rayleigh scattering of the light in the atmosphere. Because of this, constant observations of the atmosphere are conducted at the Yakutsk array during optical observation periods [14] and the obtained data on the atmospheric transparency are taken into account when determining certain characteristics of air showers, in particular, energy and depth of maximum development of the EAS [15].

The simulation algorithm also included triggers: taking into account the threshold of detectors and their fluctuations in the conditions of background illumination when measuring the flux of Cherenkov light. At the Yakutsk array, shower events are registered when one of two triggers is present: a trigger from the Cherenkov detectors of the Small Cherenkov array that registers showers with an energy of $10^{15} - 10^{17}$ eV; the second trigger is from a large array of scintillation detectors, which is triggered by the arrival of showers with energy above 10^{17} eV.

The implementation scheme of the main trigger triangles that of the Small Cherenkov array for air showers with energies of $10^{15} - 10^{18}$ eV is shown in Fig. 2.

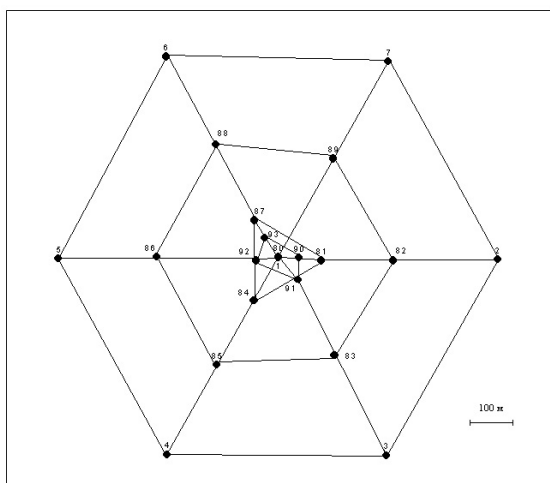


Figure 2: The configuration of trigger triangles used on the Small Cherenkov array

Since different triggers selected the events of air showers with different energies, the transition effect should affect the transition from one trigger to another. At the energy boundary, the effective collection area of showers will vary. For large showers, it is underestimated, and for small showers, on the contrary, it is overestimated. With correction of the effective area for events with high-energy showers, this effect was reduced to 15%.

4 Air Shower Energy Estimation

For showers with an energy < 500 PeV, the total number of charged particles at sea level is calculated with an accuracy of 10-25% and total flux of Cherenkov light with 10-15% accuracy. It allows one to obtain the necessary information about measured parameters of air show-

ers, which are necessary for energy estimation by calorimetry method of all EAS components observed at the array: electrons, muons, and the total Cherenkov light flux.

The data were obtained at the Small Cherenkov array for a long period, starting from 1994 to 2014 by averaging many showers in narrow intervals of energy and zenith angles.

At the Yakutsk array, the primary energy of the particle that produced the air shower is determined by the energy balance method:

$$E_0 = E_{ei} + E_{el} + E_\mu + E_{hi} + E_{\mu i} + E_\nu, \quad (1)$$

The parameters of the formula (1) were determined empirically, for energies in the range $5 \cdot 10^{15} - 3 \cdot 10^{17}$ eV (Table 2). More information about the method can be found in [12].

Table 2: The energy transferred to the different components of the EAS

n/n	lg E _{ei}	lg E _{el}	lg E _μ	lg E _{hi}	lg(E _{mi} +E _ν)	lg E ₀
1	15.687	14.506	14.840	14.465	14.721	15.823
2	15.830	14.612	14.951	14.608	14.832	15.961
3	16.064	14.876	15.175	14.842	15.056	16.195
4	16.345	15.199	15.410	15.123	15.291	16.471
5	16.540	15.362	15.506	15.318	15.387	16.650
6	16.669	15.473	15.644	15.447	15.526	16.783
7	16.797	15.726	15.783	15.575	15.664	16.916
8	16.874	15.851	15.899	15.652	15.780	17.002
9	17.014	16.001	16.015	15.792	15.896	17.139
10	17.116	16.122	16.081	15.894	15.962	17.238
11	17.208	16.269	16.173	15.986	16.054	17.334
12	17.297	16.435	16.306	16.075	16.187	17.436

The parameters Q (100), Q (200) and Q (400) weakly depend on the zenith angle. This means that the energy estimation by these parameters has less uncertainty. To determine the shower energy by these parameters, we used formulas derived empirically:

$$E_0 = (5.75 \pm 1.39) \cdot 10^{16} \cdot \left(\frac{Q(100)}{10^7} \right)^{0.96 \pm 0.03} \quad (2)$$

$$E_0 = (1.78 \pm 0.44) \cdot 10^{17} \cdot \left(\frac{Q(200)}{10^7} \right)^{1.01 \pm 0.04} \quad (3)$$

$$E_0 = (8.91 \pm 1.96) \cdot 10^{17} \cdot \left(\frac{Q(400)}{10^7} \right)^{1.03 \pm 0.05} \quad (4)$$

where Q (100), Q (200), Q (400) — Cherenkov light flux density at the distances 100, 200 and 400 m respectively.

Fig. 3 shows the dependence of E_{em}/E_0 on energy. The parameter $E_{em} = E_{ei} + E_{el}$ was determined by the formula (5) and (6) [12]. Where E_{em} is the energy transferred to the electromagnetic component, E_{ei} is the energy scattered by electrons in the atmosphere above the observation level, E_{el} is the energy carried by electrons below level of observation. In Fig. 3, the experimental data of the Yakutsk array are compared with the calculations of QGSJetII-03 [16] taken from [17].

$$E_{ei} = k(x, P_\lambda) \cdot \Phi \quad (5)$$

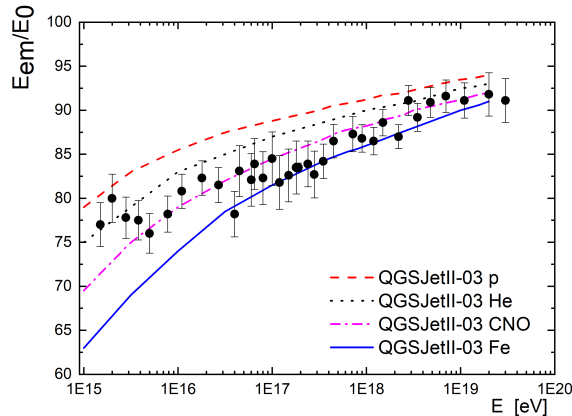


Figure 3: The fraction of energy transferred to the electromagnetic component according to the registration of Cherenkov light of EAS at the Yakutsk array and the QGSJetII-03 model of hadron interactions for the proton p (dash), helium He (dots), CNO nuclei (dash-dot) and iron Fe nucleus (solid).

Where Φ is the total flux of Cherenkov light; $k(x, P_\lambda)$ is the approximation coefficient (calculated value), taking into account the transparency of the real atmosphere, the nature of the longitudinal development of the shower (energy spectrum of secondary particles and its dependence on the age of the shower) and expressed through the depth of the maximum of EAS X_{max} , measured at the array.

$$E_{el} = 2.2 \cdot 10^6 \cdot N_s(X_0) \cdot \lambda_{eff} \quad (6)$$

where $N_s(X_0)$ is the total number of charged particles at sea level, and λ_{eff} is the absorption range of the shower particles, found from the correlation of the parameters $N_s(X_0)$ and Q (400) at different zenith angles [12].

As can be seen from Fig. 3, on average, the experimental data are consistent with calculations based on the QGSjet-03 model of hadron interactions and the mixed composition of primary particles.

5 Energy spectrum of air showers

Using the database of the Small Cherenkov array for the period from 1994 to 2014 and applying the criteria described above, we estimated the intensity of EAS events registered in a given interval in terms of the energy ΔE_i and the zenith angle $\Delta \theta_i$ per unit of the effective area of the array. The resulting spectrum is shown in Fig. 4.

As can be seen from Fig. 4a, the obtained spectrum has two features at the energy $\sim 3 \cdot 10^{15}$ eV (first knee) and at the energy $\sim 10^{17}$ eV (second knee). The first knee is characterized by the slope $\gamma_1 = 2.70 \pm 0.03$ and $\gamma_2 = 3.12 \pm 0.03$ and the second knee $\gamma_3 = 2.92 \pm 0.03$ and $\gamma_4 = 3.34 \pm 0.04$.

In Fig. 4b comparison with other experiments: TALE [18] TA BR / LR [19], KASCADE-Grande [8] and Tunka [9]. One can see a good agreement of the spectra in the energy range $10^{16} - 10^{18}$ eV. There is also a break in the spectrum at $\sim 10^{17}$ eV in other experiments as well. The spread in the spectrum is partly due to the different methods of estimating the energy at each of the EAS arrays and to some extent by the different effective thresholds of the arrays themselves. Table 3 shows comparison of spectrum slopes between different experiments.

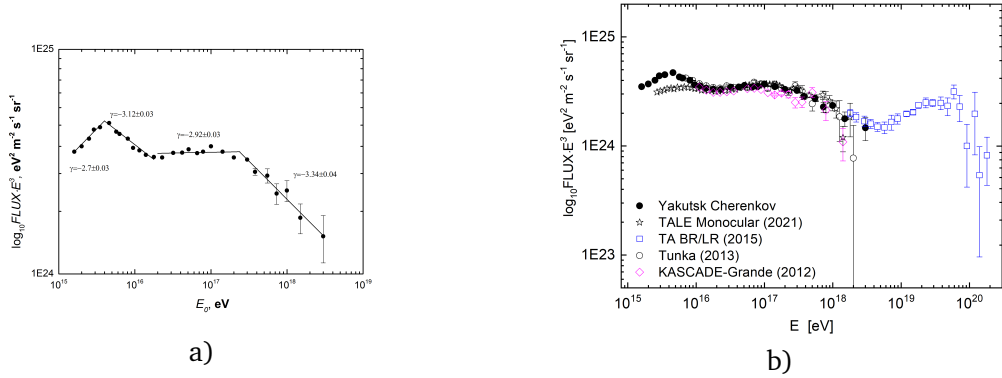


Figure 4: a) A spectrum cosmic ray in the region $10^{16} - 10^{18}$ eV by Yakutsk data b) Comparison of the spectra of the Yakutsk array (dots), TALE [18] (stars), TA-BR/LR (squares) [19], KASCADE-Grande (diamonds) [8] and Tunka (circles) [9]

Table 3: Comparison of the spectrum slopes of different experiments

Energy	Yakutsk	Tunka	KASCADE-Grande	TALE
ΔE , eV	$\gamma \pm \text{stat} \pm \text{sys}$	$\gamma \pm \text{stat} \pm \text{sys}$	$\gamma \pm \text{stat} \pm \text{sys}$	$\gamma \pm \text{stat}$
$(1.2 - 5) \cdot 10^{15}$	$-2.7 \pm 0.04 \pm 0.10$	-	-	-
$(5 - 20) \cdot 10^{15}$	$-3.12 \pm 0.03 \pm 0.07$	$-3.26 \pm 0.01 \pm 0.01$	-	-3.09 ± 0.01
$(2 - 20) \cdot 10^{16}$	$-2.92 \pm 0.03 \pm 0.06$	$-2.98 \pm 0.01 \pm 0.01$	$-2.95 \pm 0.05 \pm 0.02$	-2.89 ± 0.01
$(2 - 30) \cdot 10^{17}$	$-3.24 \pm 0.04 \pm 0.05$	$-3.35 \pm 0.01 \pm 0.01$	$-3.24 \pm 0.08 \pm 0.05$	-3.20 ± 0.02

6 Conclusion

For 20 years of continuous observations at the Yakutsk array, a large data of Cherenkov light in the energy region of $10^{16} - 10^{18}$ eV was collected. This allowed us to obtain the following results: the air shower energy was estimated by the energy balance method of all shower particles and the spectrum of cosmic rays in the energy range $10^{16} - 10^{18}$ eV is obtained. The spectrum has irregularity at the energy of $\sim 10^{17}$ eV. The slope of the spectrum changes from $\gamma_3 = 2.92 \pm 0.03$ to $\gamma_4 = 3.34 \pm 0.04$, everything indicates that at the energy of $\sim 10^{17}$ eV, the break is associated with astrophysical processes in our galaxy, as well as with extragalactic processes. The “second knee” phenomenon can be explained as transition from galactic to extragalactic cosmic rays.

Funding information This work was carried out in the framework of research project No. AAAA-A21-121011990011-8 by the Ministry of Science and Higher Education of the Russian Federation.

References

- [1] O. Adriani, G. C. Barbarino, G. A. Balizevskaya and et al., *PAMELA Measurements of Cosmic-Ray Proton and Helium Spectra*, *Science* **332**, 69 (2011), doi:[10.1126/science.1199172](https://doi.org/10.1126/science.1199172).
- [2] M. Aguilar, D. Aisa, B. Alpat and et al., *Precision Measurement of the Proton Flux in Primary Cosmic Rays from Rigidity 1 GV to 1.8 TV with the Alpha Magnetic Spec-*

trometer on the International Space Station, Phys. Rev. Lett. **114**, 171103 (2015), doi:[10.1103/PhysRevLett.114.171103](https://doi.org/10.1103/PhysRevLett.114.171103).

- [3] D. Green and E. A. Hays, *Measurement of the Cosmic-ray Proton Spectrum with the Fermi Large Area Telescope*, Proc. of Sci. **301**, 159 (2018), doi:[10.22323/1.301.0159](https://doi.org/10.22323/1.301.0159).
- [4] A. Panov, J. A. Jr., H. Ahn and et al., *Energy spectra of abundant nuclei of primary cosmic rays from the data of ATIC-2 experiment: Final results*, Bull. of the RAoS: Physics **73**, 564 (2009), doi:[10.3103/S1062873809050098](https://doi.org/10.3103/S1062873809050098).
- [5] E. Seo, H. Ahn, P. Allison and et al., *CREAM: 70 days of flight from 2 launches in Antarctica*, Adv. Space Res. **42**, 1656 (2008), doi:[10.1016/j.asr.2007.03.056](https://doi.org/10.1016/j.asr.2007.03.056).
- [6] A. Aab, P. Abreu, M. Aglietta and et al., *The Pierre Auger Cosmic Ray Observatory*, NIM A **798**, 172 (2015), doi:[10.1016/j.nima.2015.06.058](https://doi.org/10.1016/j.nima.2015.06.058).
- [7] T. Abu-Zayyad, R. Aida, M. Allen and et al., *The surface detector array of the Telescope Array experiment*, NIM A **689**, 87 (2012), doi:[10.1016/j.nima.2012.05.079](https://doi.org/10.1016/j.nima.2012.05.079).
- [8] W. Apel, J. Arteaga-Velazquez, K. Bekk and et al., *The spectrum of high-energy cosmic rays measured with KASCADE-Grande*, Astropart. Phys. **36**, 183 (2012), doi:[10.1016/j.astropartphys.2012.05.023](https://doi.org/10.1016/j.astropartphys.2012.05.023).
- [9] V. Prosin, S. Berezhnev, N. Budnev and et al., *Tunka-133: Results of 3 year operation*, NIM A **756**, 94 (2014), doi:[10.1016/j.nima.2013.09.018](https://doi.org/10.1016/j.nima.2013.09.018).
- [10] S. Knurenko, V. Kolosov and Z. Petrov, *Cerenkov radiation of cosmic ray extensive air showers. Part 3. Longitudinal development of showers in the energy region of $10^{15} - 10^{17}$ eV*, 27 ICRC (Hamburg) **1**, 157 (2001).
- [11] S. Knurenko, V. Kolosov, Z. Petrov and et al., Sci. and Edu. **4**, 46 (1998).
- [12] S. Knurenko, A. Ivanov, I. Sleptsov and A. Sabourov, *Estimation of the energy of the electron-photon component of cosmic rays on the basis of data for Cherenkov light from ultrahigh-energy extensive air showers*, JETP Lett. **83**, 473 (2006), doi:[10.1134/S0021364006110014](https://doi.org/10.1134/S0021364006110014).
- [13] S. Knurenko, Z. Petrov and I. Petrov, *Second knee on the spectrum of cosmic ray at energies $\sim 10^{17}$ ev by long-termn observations of small cherenkov eas array*, Physics of Atomic Nuclei **82**, 732 (2019), doi:[10.1134/S106377881966027X](https://doi.org/10.1134/S106377881966027X).
- [14] S. Knurenko and I. S. Petrov, *Atmospheric circulation influence during winter on change of air pressure, temperature and spectral transparency at Yakutsk Array*, Proc. SPIE **9292**, 92925B (2014), doi:[10.1117/12.2074877](https://doi.org/10.1117/12.2074877).
- [15] S. Knurenko and I. S. Petrov, *Comparison of the relative transparency of the atmosphere measured by attenuation of Cherenkov light*, Proc. SPIE **10466**, 1046659 (2017), doi:[10.1117/12.2286013](https://doi.org/10.1117/12.2286013).
- [16] S. Ostapchenko, *QGSJET-II: towards reliable description of very high energy hadronic interactions*, Nucl. Phys. B, Proc. Suppl. **151**(1), 143 (2006), doi:[10.1016/j.nuclphysbps.2005.07.026](https://doi.org/10.1016/j.nuclphysbps.2005.07.026).
- [17] R. U. Abbasi, M. Abe, T. Abu-Zayyad and et al., *The Cosmic Ray Energy Spectrum between 2 PeV and 2 EeV Observed with the TALE Detector in Monocular Mode*, ApJ **865**, 74 (2018), doi:[10.3847/1538-4357/aada05](https://doi.org/10.3847/1538-4357/aada05).

- [18] T. Abu-Zayyad, R. Abbasi, M. Allen and et al, *Cosmic ray energy spectrum measured by the tale fluorescence detector*, PoS **395**, 347 (2022), doi:[10.22323/1.395.0347](https://doi.org/10.22323/1.395.0347).
- [19] R. Abbasi, M. Abe, T. Abu-Zayyad and et al, *The energy spectrum of cosmic rays above $10^{17.2}$ eV measured by the fluorescence detectors of the Telescope Array experiment in seven years*, Astropart. Phys. **80**, 131 (2016), doi:[10.1016/j.astropartphys.2016.04.002](https://doi.org/10.1016/j.astropartphys.2016.04.002).